Supplemental Information

Parallel Metabolomic Profiling of Cerebrospinal Fluid and Serum for Identifying Biomarkers of Injury Severity after Acute Human Spinal Cord Injury

Yiman Wu[1], Femke Streijger[2], Yining Wang[3], Guohui Lin[3], Sean Christie[4], Jean-Marc Mac-Thiong[5], Stefan Parent[6], Christopher S. Bailey[7], Scott Paquette[8], Michael C. Boyd[8], Tamir Ailon[8], John Street[9], Charles G. Fisher[9], Marcel F. Dvorak[9], Brian K. Kwon[2]*, Liang Li[1]*

1. Department of Chemistry, University of Alberta, Edmonton, AB T6G2G2, Canada
2. International Collaboration on Repair Discoveries (ICORD), University of British Columbia, Blusson Spinal Cord Centre, 818 West 10th Avenue, Vancouver, BC, V5Z 1M9, Canada
3. Department of Computing Science, University of Alberta, Edmonton, AB, T6T 2E8, Canada
4. Division of Neurosurgery, Dalhousie University, Halifax Infirmary, 1796 Summer Street, Halifax, NS, B3H 3A7, Canada
5. Hôpital du Sacré-Coeur de Montréal, 5400 Boul Gouin O, Montréal, QC, H4J 1C5, Canada
6. Chu Sainte-Justine, Dept. of Surgery, Université de Montréal, PO Box 6128, Station Centre-ville, Montreal, QC, H3C 3J7, Canada
7. Division of Orthopaedic Surgery, Schulich Medicine & Dentistry, Victoria Hospital 800 Commissioners Road East, Room E4 120, London, ON, N6C 5W9, Canada
8. Division of Neurosurgery, University of British Columbia, Vancouver Spine Surgery Institute, 818 West 10th Avenue, Vancouver, BC, V5Z 1M9, Canada
9. Department of Orthopaedics, University of British Columbia, Vancouver Spine Surgery Institute, 818 West 10th Avenue, Vancouver, BC, V5Z 1M9, Canada

Supplemental Note S1. CIL LC-MS Metabolomic Profiling and Performance Evaluation

1. Overview of metabolomic profiling workflow

Figure 1 in the main text illustrates the overall differential isotope labeling metabolomic profiling workflow. In this workflow, CSF and serum samples were analyzed in parallel. CSF and serum metabolites were extracted via protein precipitation with three volumes of MeOH. After extraction, the total solution volume is 100 μL. However, because serum contains a large amount of protein precipitates, in practice, we recommend that only 75 μL of the serum supernatant to be taken in order to avoid the precipitate. On the other hand, the protein content in CSF is small, and therefore 90 μL of the CSF supernatant can be taken without having the precipitate in the solution. Prior to LC-MS analysis, each ^{12}C-labeled individual CSF or serum sample was combined with an equal amount of the corresponding ^{13}C-labeled pooled reference sample. The LC-MS data was processed by IsoMS[1] to extract peak ratio information for each individual peak pair found in the mass spectra, and the missing values were retrieved using the zero-fill program[2]. Finally the processed data was subjected to statistical analysis for discovery of differentiating metabolites. Since each sample was only analyzed once (i.e., no experimental replicates), it is important to ensure a good peak detectability and repeatability of this analytical platform. Therefore, these parameters were first examined prior to the metabolomic profiling analysis.

2. Evaluation of the Analytical Platform

To evaluate the analytical variability, the coefficient of variation (CV) was determined from three experimental replicates that is a combination of variations introduced during protein

precipitation, labeling, solution mixing, LC-MS detection and data processing. The CV values were calculated by using peak ratios of all peak pairs commonly detected in three replicate runs. Table 1 lists the median and average CV values for each sample. For all eight samples, the median CVs were less than 15% and the mean CVs were of 17% or less. In addition to determination of the CV values, we also examined the percentage of commonly detected peak pairs from experimental triplicates. The non-common peak pairs, or missing values, in replicate runs are usually caused by the presence of borderline metabolites, false positive peak pair identification, or other situations in which the peak picking criteria are not met (e.g., large retention time or mass shift). Therefore, the percentage of common peak pairs reflects both the reproducibility of measurements and the robustness of the data analysis procedure. Figure 1 shows the number distributions of the peak pairs found in three experimental replicates for all eight samples. The percentage overlap of detected metabolites between three experimental replicates was over 92% for all samples examined, suggesting a good reproducibility of this analytical platform. The analytical variability is very similar in CSF and serum based on this differential isotope labeling approach.

Table 1. Measured analytical variations in CSF and serum samples

Biofluid	Sample group	Mean CV (%)	Median CV (%)
CSF	AIS A	17	12
	AIS B	13	11
	AIS C	17	14
	Control	16	14
Serum	AIS A	16	12
	AIS B	17	14
	AIS C	16	12
	Control	17	14

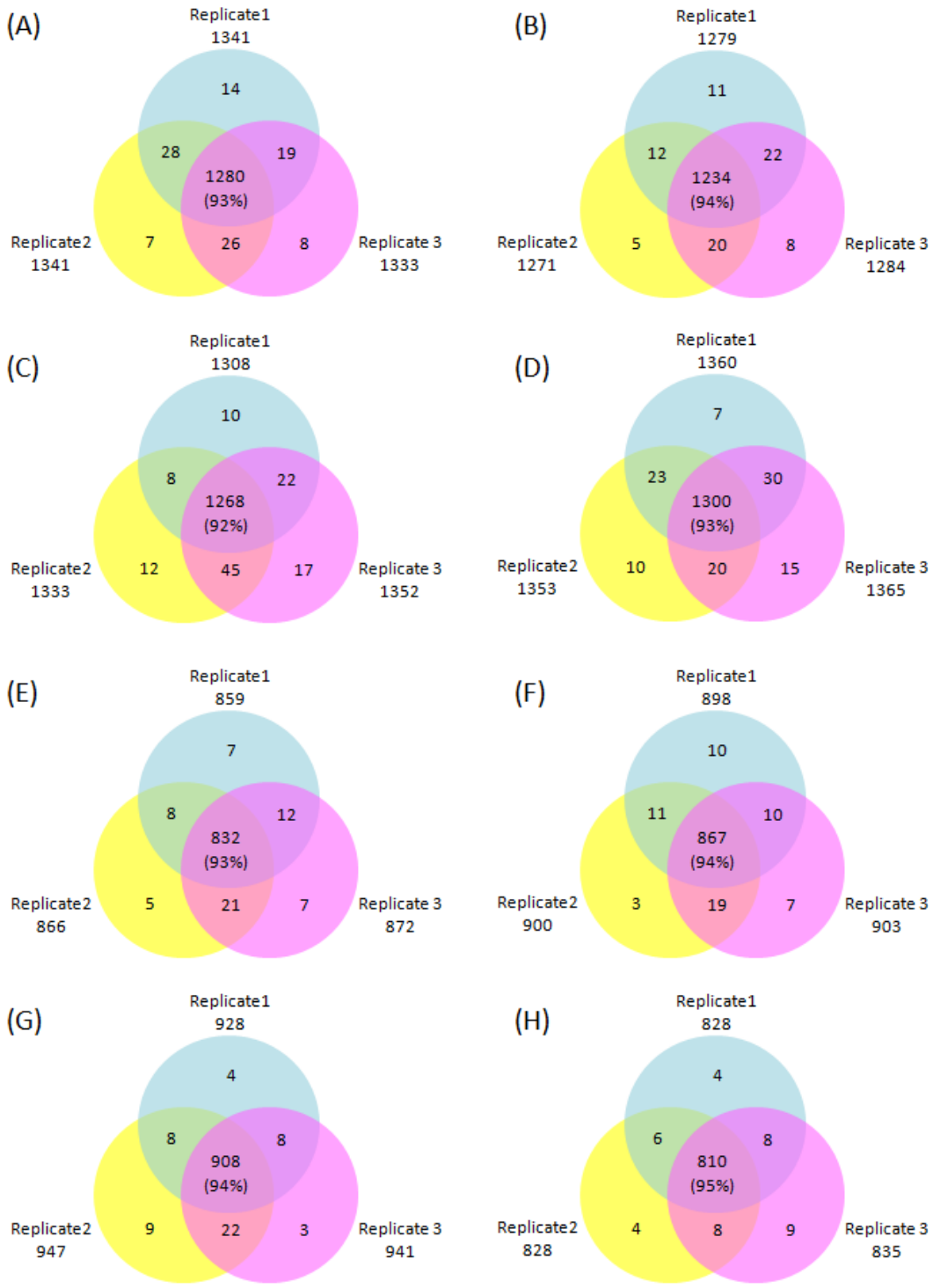

Figure 1. Distributions of the number of peak pairs detected in three experimental replicates for (A) serum AIS A; (B) serum AIS B; (C) serum AIS C; (D) serum control; (E) CSF AIS A; (F) CSF AIS B; (G) CSF AIS C; (H) CSF control.

In LC-MS analysis, the sample injection amount plays an important role on the number of metabolites detected. For small injection amounts, metabolites with concentrations close to the instrument detection threshold (known as borderline metabolites)[3] may not be detected. On the other hand, with large injection amounts, signals from low abundance metabolites co-eluting with a high intensity metabolite may be suppressed. Moreover, column saturation and sample carryover problems may occur. In this work, we examined the relationship between the number of peak pairs detected and the injection volume using the pooled CSF and serum samples (Figure 2). The injection amount can be calculated by multiplying the injection volume with the nominal total metabolite concentrations of CSF and serum determined from the calibration curve established with a mixture of 17 amino acid standards[4,5]. For CSF, the number of peak pairs increases by 20% when the injection volume increases from 6 μL to 12 μL, and then levels off. This significant increase in the number of peak pairs is likely attributed to the low metabolite concentration levels in CSF samples, since many of the borderline metabolites cannot be detected when the injection amount is not sufficiently high. In contrast, by increasing the injection volume from 6 μL to 10 μL, the number of peak pairs increases only by 5%, and further increase in the injection volume leads to a decrease in the peak pair number. Compared to CSF, the metabolite levels in serum are considerably higher, and consequently the percentage of borderline metabolites is smaller. On the other hand, at higher injection amounts, ion suppression from high abundance ions becomes noticeable in serum samples[6]. The effect of ion suppression at higher injection amounts is illustrated in Figure 3. In this example, the signals of the low abundance peak pair 318.560 and 320.567 increases when the injection volume increases from 6 μL to 8 μL, and decreases as the injection volume increases further. At an injection volume of 14

μL, this peak pair falls below the detection threshold and becomes non-detectable. Considering both effects (borderline metabolites and ion suppression), the optimal injection amount was chosen as the point at which the number of peak pairs levels off or starts to decrease. Based on Figure 3, the optimal injection volume was determined to be 12 μL for CSF and 10 μL for serum (the corresponding injection amount was 3.3 nmole and 5.7 nmole), which gave 1213 and 2316 peak pairs for CSF and serum, respectively. It is not surprising to see a smaller number of metabolites in CSF compared to serum. As the primary carrier of small molecules in the body, the metabolite composition in serum is much more complex than CSF, and it also contains a greater number of exogenous compounds.

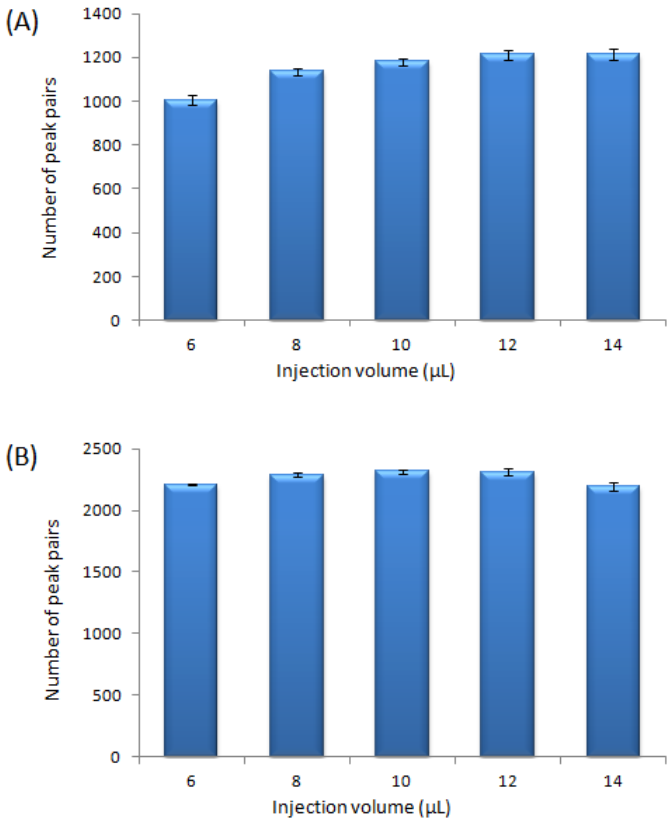

Figure 2. Plot of the number of peak pairs detected against the injection volume for (A) CSF and (B) serum.

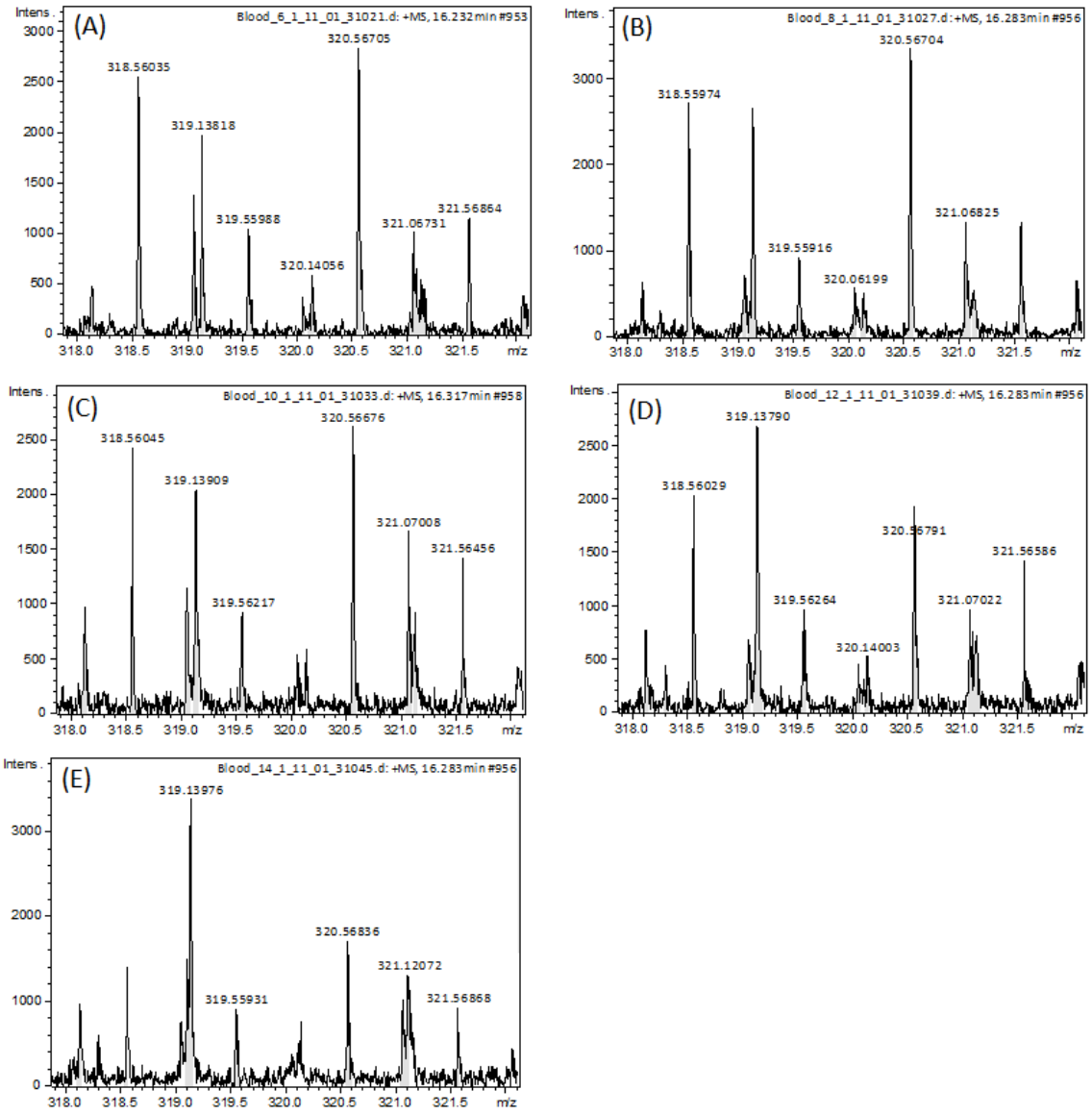

Figure 3. An example showing ion suppression effect with larger injection amounts for the peak pair 318.560 and 320.567. The injection amounts are (A) 6 μL; (B) 8 μL; (C) 10 μL; (D) 12 μL and (E) 14 μL.

3. Comparison of the CSF and Serum Metabolome

Figure 4 shows the overlaid base-peak ion chromatograms (BPCs) for CSF and serum. Most of the high abundance peaks correspond to labeled amino acids (indicated by stars). It is noted that while the majority of the peaks were common to CSF and serum, the metabolite intensity in serum is much higher than that in CSF. For example, among the fifteen identified amino acids in Figure 4, only glutamine gives higher signal in CSF compared to serum, while all the other fourteen amino acids have much higher abundance in serum. In addition, since serum is a lipid rich biofluid, we also observed several phospholipid peaks in the BPC of serum (labeled with dots), which were barely detectable in CSF. These unlabeled compounds appear as singlet peaks in the mass spectra and therefore will not be considered in the current metabolomic profiling workflow.

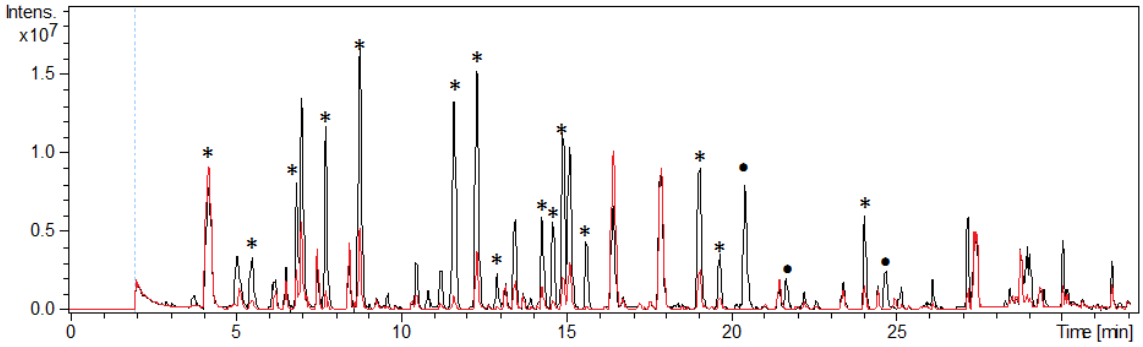

Figure 4. Base-peak ion chromatograms of CSF (red) and serum (black). Peaks labeled with a star correspond to amino acids, and peaks labeled with a dot correspond to phospholipids. The first amino acid peak (eluted out at 4 min) is glutamine.

The BPC only shows metabolites with the greatest signal intensities. To compare the relative quantities of all metabolites common to CSF and serum, a "pooled pool" reference sample was generated by combining the pooled CSF and serum samples and then labeled with ^{13}C dansyl chloride. The ^{12}C-labeled CSF and serum pool samples were combined with the ^{13}C-

labeled “pooled pool” reference in 1:1 volume ratio, so that the relative intensities of individual metabolites can be assessed based on the ^{12}C to ^{13}C peak ratios of each peak pair. Supplemental Figure 5 shows a scatter plot that compares the relative metabolite intensities in CSF and serum. For more than half of the peak pairs, the $^{12}C/^{13}C$ peak ratio is larger in serum than in CSF, indicating higher metabolite concentration in serum. In contrast, only less than 30% of the metabolites have higher concentrations in CSF. Moreover, there are a number of data points located along the y = x curve, which correspond to metabolites that have similar intensities in CSF and serum.

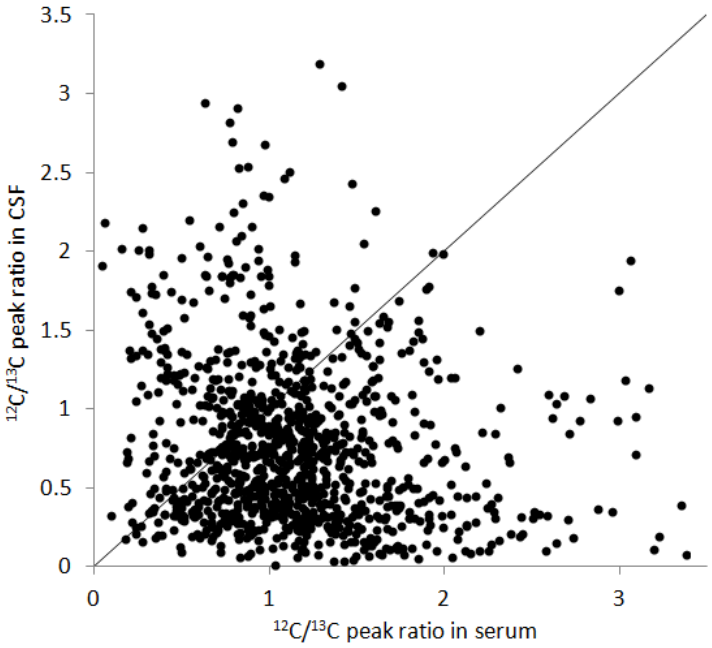

Figure 5. Comparison between the relative metabolite intensities in serum and CSF, expressed as $^{12}C/^{13}C$ peak ratios. Each dot represents a peak pair (or putative metabolite).

While CSF is often considered as an ideal biofluid for studying neurological disorders, the low metabolite concentration in CSF can pose a challenge to the biomarker discovery process, as the concentrations of some biologically meaningful metabolites may fall below the instrument

detection limit. For example, we found that serotonin, an important neurotransmitter, was not detected in CSF. On the other hand, the higher overall metabolite concentration in serum allows for more sensitive detection and identification of biomarkers. In addition, serum also has the advantage of easy accessibility, which makes it an attractive alternative for studying central nervous system disorders[7]. Nevertheless, some of the metabolites can only be detected in CSF (e.g., the brain-specific dipeptide homocarnosine). Also, since the matrix is more complex in serum, the detectability of low intensity metabolites can be compromised by ion suppression. For investigating metabolic changes associated with these compounds, analysis of CSF is the better approach. Therefore, the selection of the biofluid type plays an important role in the biomarker discovery process, and the choice is dependent on the objective of study, sample availability, instrument sensitivity and the metabolites of interest. Parallel metabolomic profiling of CSF and serum on a small pilot set may be carried out to assist selection of the biofluid.

References

1 Zhou, R., Tseng, C.L., Huan, T., & Li, L., IsoMS: automated processing of LC-MS data generated by a chemical isotope labeling metabolomics platform. *Anal Chem* 86 (10), 4675-4679 (2014).

2 Huan, T. & Li, L., Counting missing values in a metabolite-intensity data set for measuring the analytical performance of a metabolomics platform. *Anal Chem* 87 (2), 1306-1313 (2015).

3 Chen, Y. *et al.*, Combination of injection volume calibration by creatinine and MS signals' normalization to overcome urine variability in LC-MS-based metabolomics studies. *Anal Chem* 85 (16), 7659-7665 (2013).

[4] Wu, Y. & Li, L., Determination of total concentration of chemically labeled metabolites as a means of metabolome sample normalization and sample loading optimization in mass spectrometry-based metabolomics. *Anal Chem* 84 (24), 10723-10731 (2012).

[5] Xu, W. *et al.*, Development of high-performance chemical isotope labeling LC-MS for profiling the human fecal metabolome. *Anal Chem* 87 (2), 829-836 (2015).

[6] Zhou, R.K. & Li, L., Effects of sample injection amount and time-of-flight mass spectrometric detection dynamic range on metabolome analysis by high-performance chemical isotope labeling LC-MS. *J. Proteomics* 118, 130-139 (2015).

[7] Quinones, M.P. & Kaddurah-Daouk, R., Metabolomics tools for identifying biomarkers for neuropsychiatric diseases. *Neurobiol Dis* 35 (2), 165-176 (2009).

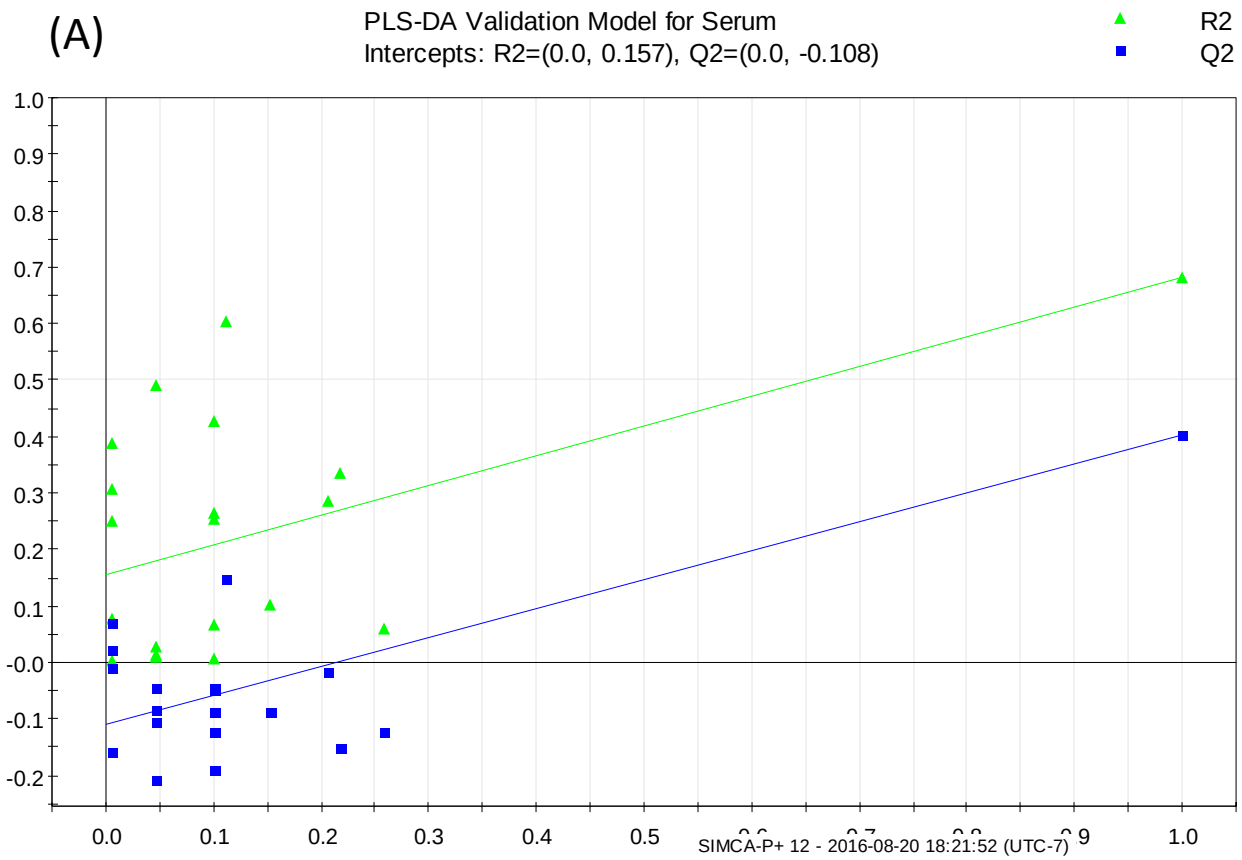

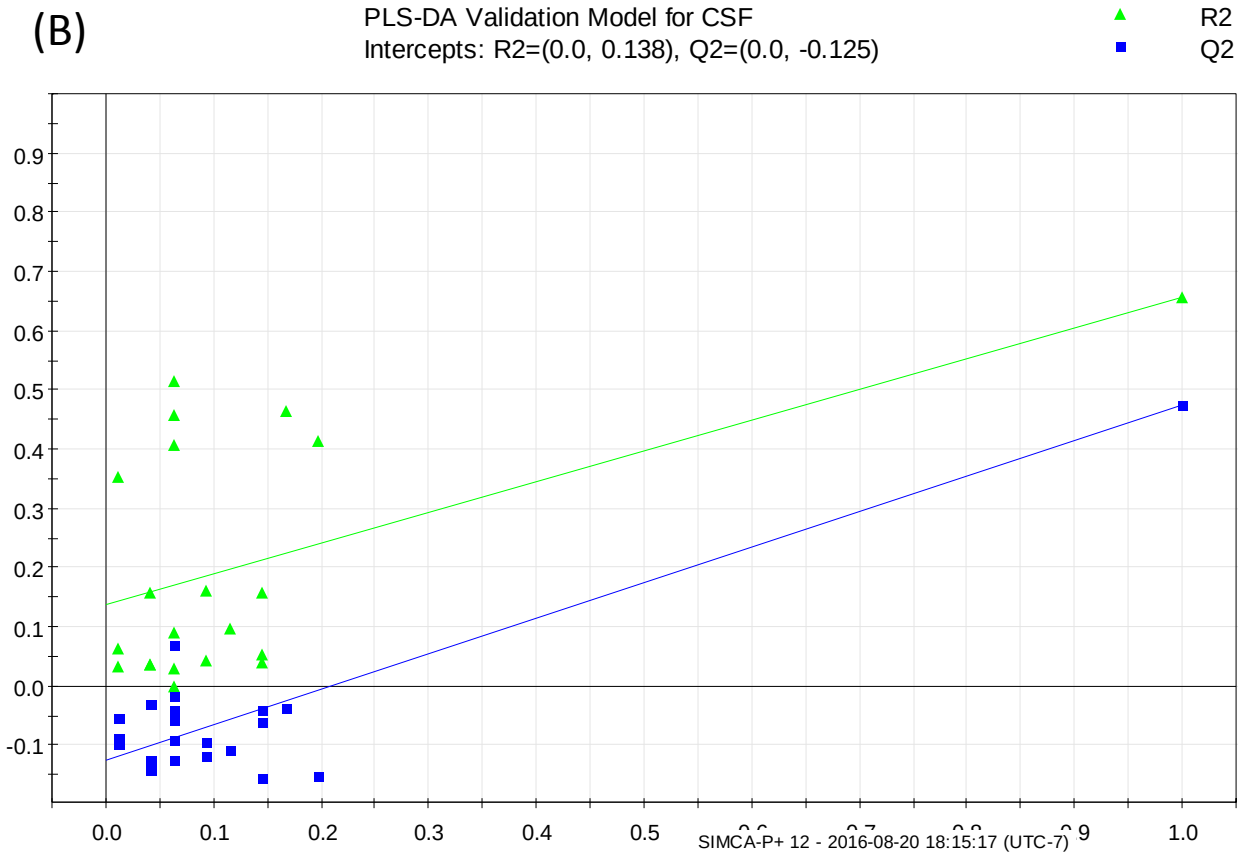

Supplemental Figure S1. Validation of PLS-DA models for (A) serum and (B) CSF data sets using twenty-permutation test.

Supplemental Tables T1-T8

Supplemental Table T1. List of metabolites positively identified based on retention time and mass matches to those of metabolite standards.

HMDB.No.	Name	Accurate mass	mz_light	Retention time (min)	mz difference (ppm)	rt difference (s)	Note
HMDB01414	1,4-diaminobutane	88.1000	278.1083	21.39	2.10	4.0	
HMDB02362	2,4-Diaminobutyric acid	118.0742	293.0954	15.85	0.45	5.5	
HMDB01123	2-Aminobenzoic acid	137.0477	371.1060	16.78	4.32	2.1	
HMDB00991	2-aminooctanoic acid	159.1259	393.1842	19.10	0.33	11.1	
HMDB02210	2-Phenylglycine	151.0633	385.1216	12.02	2.52	7.5	
HMDB01336	3,4-Dihydroxybenzeneacetic acid	168.0423	318.0794	23.86	2.34	3.0	
HMDB03911	3-Aminoisobutanoic acid	103.0633	337.1216	8.96	0.90	1.9	
HMDB02390	3-Cresotinic acid	152.0473	386.1057	17.06	2.37	8.1	
HMDB00750	3-Hydroxymandelic acid	168.0423	402.1006	13.37	0.17	14.8	
HMDB00750_2	3-Hydroxymandelic acid - COOH	168.0423	356.0951	21.80	1.34	7.0	
HMDB00440	3-Hydroxyphenylacetic acid	152.0473	386.1057	16.71	2.21	8.0	
HMDB00022	3-Methoxytyramine or Phenylephrine	167.0946	317.6056	25.50	0.39	1.7/7.7	
HMDB00479	3-methyl-histidine or 1-Methylhistidine	169.0851	403.1434	2.41	0.86	2.5/7.1	
HMDB01169_2	4-Aminophenol - multi-tags	109.0528	288.5847	25.40	3.39	22.5	
HMDB29306	4-Ethylphenol	122.0732	356.1315	25.84	1.01	13.9	
HMDB00500	4-Hydroxybenzoic acid	138.0317	372.0900	17.75	2.30	4.4	
HMDB01232	4-Nitrophenol	139.0269	373.0853	23.61	1.69	8.9	
HMDB01149	5-Aminolevulinic acid	131.0582	365.1166	7.88	3.04	1.0	
HMDB03355	5-Aminopentanoic acid	117.0790	351.1373	9.10	1.28	9.8	
HMDB00763	5-Hydroxyindoleacetic acid	191.0582	425.1166	15.38	0.39	8.3	
HMDB00450	5-Hydroxylysine	162.1004	315.1085	13.85	0.62	12.4	
HMDB00469	5-Hydroxymethyluracil	142.0378	376.0962	9.56	1.14	26.8	
HMDB01859	Acetaminophen	151.0633	385.1216	16.57	2.58	5.5	
HMDB00050	Adenosine	267.0968	501.1551	4.42	0.20	9.4	
HMDB00510	Aminoadipic acid	161.0688	395.1271	6.25	1.97	1.0	
HMDB03012	Aniline	93.0578	327.1162	17.72	0.73	17.2	
HMDB00056	Beta-Alanine	89.0477	323.1060	7.49	0.82	1.7	
HMDB02322	Cadaverine	102.1157	285.1162	22.62	1.13	11.6	
HMDB00904	Citrulline	175.0957	409.1540	3.79	1.46	17.4	
HMDB02199	Desaminotyrosine	166.0630	400.1213	18.11	0.28	2.1	Only detected in serum
HMDB00070	D-Pipecolic acid	129.0790	363.1373	13.45	2.12	2.5	
HMDB00149	Ethanolamine	61.0528	295.1111	6.44	1.93	8.8	
HMDB00112	Gamma-Aminobutyric acid	103.0633	337.1216	7.94	0.43	7.2	
HMDB00152	Gentisic acid	154.0266	388.0849	17.43	1.44	12.3	
HMDB00152_2	Gentisic acid - multi-tags	154.0266	311.0716	24.78	3.06	5.4	
HMDB00131	Glycerol	92.0473	280.0820	22.91	0.71	0.5	
HMDB00123	Glycine	75.0320	309.0903	6.95	1.72	4.5	
HMDB00721	Glycylproline	172.0848	406.1431	7.43	0.69	1.3	
HMDB01398	Guaiacol	124.0524	358.1107	22.76	1.43	11.5	
HMDB01842	Guanidine	59.0483	293.1067	3.17	3.77	10.9	Only detected in CSF
HMDB00133	Guanosine	283.0917	517.1500	2.49	1.20	5.4	
HMDB00745	Homocarnosine	240.1222	354.1194	17.41	0.69	11.6	Only detected in CSF
HMDB00130	Homogentisic acid	168.0423	318.0794	24.83	0.15	0.5	Only detected in serum
HMDB00670	Homo-L-arginine	188.1273	422.1856	3.26	0.19	5.0	
HMDB00118	Homovanillic acid	182.0579	416.1162	16.86	1.52	13.2	
HMDB00755	Hydroxyphenyllactici acid	182.0579	416.1162	14.74	0.53	11.2	
HMDB00157_3	Hypoxanthine - Isomer	136.0385	370.0968	10.00	1.52	6.5	
HMDB00157_2	Hypoxanthine - multi-tags	136.0385	370.0968	8.98	1.56	0.2	
HMDB00157	Hypoxanthine + H2O	136.0385	388.1098	2.54	3.94	3.5	
HMDB02024	Imidazoleacetic acid	126.0429	360.1012	11.28	1.64	3.4	
HMDB03320	Indole-3-carboxylic acid	161.0477	395.1060	19.30	0.76	3.6	
HMDB00734	Indoleacrylic acid	187.0633	421.1216	21.02	2.27	21.3	Only detected in serum
HMDB60003	Isovanillic acid	168.0423	402.1006	15.64	2.98	11.9	
HMDB00704	Isoxanthopterin	179.0443	413.1026	9.77	0.62	1.1	
HMDB00190	Lactic acid	90.0317	324.0900	11.96	1.54	0.9	
HMDB00161	L-Alanine	89.0477	323.1060	7.90	1.54	3.3	
HMDB00452	L-Alpha-aminobutyric acid	103.0633	337.1216	9.48	2.61	6.5	
HMDB00517	L-Arginine	174.1117	408.1700	2.70	0.54	5.6	
HMDB00168	L-Asparagine	132.0535	366.1118	3.25	3.34	5.6	
HMDB00191	L-Aspartic Acid	133.0375	367.0958	5.45	3.42	1.3	
HMDB00706	L-Aspartyl-L-phenylalanine	280.1059	514.1642	10.78	1.43	28.9	
HMDB00099_2	L-Cystathionine - Isomer	222.0674	345.0920	13.87	0.10	0.3	
HMDB00192	L-Cystine	240.0238	354.0702	14.17	2.38	6.6	
HMDB00148	L-Glutamic Acid	147.0532	381.1115	5.32	3.97	2.5	
HMDB00148_2	L-Glutamic Acid - H2O	147.0532	363.1009	9.71	3.01	0.5	
HMDB00641	L-Glutamine	146.0691	380.1275	3.72	2.75	3.6	
HMDB00177	L-Histidine	155.0695	389.1278	18.20	2.48	0.4	
HMDB00719	L-Homoserine	119.0582	353.1166	4.51	2.30	8.2	
HMDB00719_2	L-Homoserine - H2O	119.0582	335.1060	9.71	0.90	12.7	
HMDB00172	L-Isoleucine	131.0946	365.1529	13.25	2.78	0.3	
HMDB00687	L-leucine	131.0946	365.1529	13.54	2.53	0.0	
HMDB00182	L-Lysine	146.1055	307.1111	17.50	0.72	5.3	
HMDB00696	L-Methionine	149.0510	383.1094	11.26	2.63	9.5	
HMDB00159	L-Phenylalanine	165.0790	399.1373	13.06	2.01	8.1	
HMDB00162	L-Proline	115.0633	349.1216	10.54	2.45	8.1	
HMDB00187	L-Serine	105.0426	339.1009	4.71	3.04	1.1	
HMDB00167	L-Threonine	119.0582	353.1166	6.12	2.83	1.6	
HMDB00929	L-Tryptophan	204.0899	438.1482	11.65	1.29	0.0	
HMDB00158	L-Tyrosine	181.0739	324.5953	22.67	0.39	0.9	
HMDB00883	L-Valine	117.0790	351.1373	11.19	2.73	9.8	

HMDB02048	m-Cresol	108.0575	342.1158	24.58	2.69	8.3	
HMDB02005	Methionine Sulfoxide	165.0460	399.1043	3.94	2.23	7.0	
HMDB02005_2	Methionine Sulfoxide - Isomer	165.0460	399.1043	4.38	1.12	9.2	
HMDB02108	Methylcysteine	135.0354	369.0937	9.80	1.43	11.4	
HMDB01522	Methylguanidine	73.0640	307.1223	4.34	0.56	10.1	
HMDB02172	N1,N12-Diacetylspermine	286.2369	377.1768	14.82	1.20	0.9	
HMDB02064	N-Acetylputrescine	130.1106	364.1689	7.37	1.74	9.5	
HMDB00446	N-Alpha-acetyllysine	188.1161	422.1744	7.23	0.21	9.6	
HMDB02141	N-Methyl-a-aminoisobutyric acid	117.0790	351.1373	13.97	3.88	9.1	
HMDB02393	N-methyl-D-aspartic acid	147.0532	381.1115	8.03	0.18	13.8	
HMDB02055	o-Cresol	108.0575	342.1158	24.80	1.37	12.3	
HMDB00224	O-Phosphoethanolamine	141.0191	375.0774	2.14	1.90	15.0	
HMDB00214	Ornithine	132.0899	300.1033	16.64	2.28	4.4	
HMDB03337	Oxidized glutathione	612.1520	540.1343	8.16	3.05	10.4	
HMDB01392	p-Aminobenzoic acid	137.0477	371.1060	11.63	4.31	5.8	
HMDB00210	Pantothenic acid	219.1107	453.1690	8.53	1.25	6.2	
HMDB00228	Phenol	94.0419	328.1002	23.51	0.73	19.9	
HMDB13302	Phenylalanylphenylalanine	312.1474	546.2057	16.59	0.50	5.3	Only detected in serum
316	Phenyl-Leucine	278.1631	512.2214	15.91	3.38	7.9	Only detected in serum
HMDB00020	p-Hydroxyphenylacetic acid	152.0473	386.1057	17.26	1.65	14.1	
HMDB01545	Pyridoxal	167.0582	401.1166	12.38	2.42	10.4	
HMDB00884_3	Ribothymidine - H2O	258.0852	474.1329	9.68	1.53	2.9	
HMDB00884_2	Ribothymidine - Isomer	258.0852	492.1435	8.70	0.51	5.7	
HMDB00279	Saccharopine	276.1321	510.1905	2.60	2.20	1.2	
HMDB00279_2	Saccharopine - H2O	276.1321	492.1799	5.99	1.36	2.2	
HMDB01895	Salicylic acid	138.0317	372.0900	15.86	1.39	6.1	
HMDB00840	Salicyluric acid	195.0532	429.1115	11.29	0.08	1.3	Only detected in serum
HMDB00271	Sarcosine	89.0477	323.1060	9.65	0.93	3.7	
HMDB00259	Serotonin	176.0950	322.1058	24.85	3.97	12.1	Only detected in serum
HMDB03334	Symmetric dimethylarginine	202.1430	436.2013	3.52	0.41	7.4	
HMDB00251	Taurine	125.0147	359.0730	2.58	2.31	0.9	
HMDB01918	Thyroxine	776.6867	622.4017	27.68	0.11	0.4	Only detected in serum
HMDB00725	Trans-4-Hydroxyl-L-Proline	131.0582	365.1166	5.44	3.07	2.3	
HMDB00300	Uracil	112.0273	346.0856	11.81	1.30	15.6	
HMDB00296	Uridine	244.0695	478.1279	8.13	1.69	1.1	
HMDB00296_2	Uridine - H2O	244.0695	460.1173	8.89	1.06	2.3	
HMDB00301	Urocanic acid	138.0429	372.1012	13.70	0.41	0.2	
HMDB00484	Vanillic acid	168.0423	402.1006	17.79	0.20	20.4	
HMDB00291	Vanillylmandelic acid	198.0528	432.1111	13.02	1.14	1.5	
HMDB00292	Xanthine	152.0334	386.0917	9.33	1.68	7.9	

Supplemental Table T2. Summary of pathway analysis results.

Pathway Name from CSF Data	Total	Hits	Raw *p*	-log(*p*)	Impact
Pyrimidine metabolism	60	1	1.10E-07	16.02	0.02
Aminoacyl-tRNA biosynthesis	75	5	9.39E-06	11.58	0.06
Arginine and proline metabolism	77	6	1.87E-05	10.89	0.27
Histidine metabolism	44	1	9.40E-05	9.27	0.05
Lysine biosynthesis	32	1	2.39E-04	8.34	0.10
Biotin metabolism	11	1	2.39E-04	8.34	0.00
D-Arginine and D-ornithine metabolism	8	1	2.80E-04	8.18	0.00
Lysine degradation	47	2	4.99E-04	7.60	0.16
Glycine, serine and threonine metabolism	48	2	7.29E-04	7.22	0.10
Valine, leucine and isoleucine biosynthesis	27	2	1.19E-03	6.73	0.01
Glycerophospholipid metabolism	39	1	1.90E-03	6.26	0.06
Nitrogen metabolism	39	2	2.25E-03	6.10	0.00
Porphyrin and chlorophyll metabolism	104	1	2.93E-03	5.83	0.00
Pyruvate metabolism	32	1	3.90E-03	5.55	0.14
Glycolysis or Gluconeogenesis	31	1	3.90E-03	5.55	0.00
Propanoate metabolism	35	1	3.90E-03	5.55	0.00
Tryptophan metabolism	79	2	5.53E-03	5.20	0.07
Phenylalanine, tyrosine and tryptophan biosynthesis	27	1	1.02E-02	4.58	0.07
Valine, leucine and isoleucine degradation	40	1	1.31E-02	4.33	0.00
Cysteine and methionine metabolism	56	1	1.80E-02	4.02	0.13
Glycerolipid metabolism	32	1	2.36E-02	3.75	0.19
Galactose metabolism	41	1	2.36E-02	3.75	0.00
Alanine, aspartate and glutamate metabolism	24	1	5.05E-02	2.99	0.10
Butanoate metabolism	40	1	5.05E-02	2.99	0.01
beta-Alanine metabolism	28	1	5.05E-02	2.99	0.00
Glutathione metabolism	38	2	8.27E-02	2.49	0.00
Pathway Name from Serum Data	**Total**	**Hits**	**Raw *p***	**-log(*p*)**	**Impact**
Pyrimidine metabolism	60	1	4.79E-07	14.55	0.02
Phenylalanine metabolism	45	1	1.15E-05	11.37	0.12
Phenylalanine, tyrosine and tryptophan biosynthesis	27	1	1.15E-05	11.37	6.2E-04
Nitrogen metabolism	39	1	1.15E-05	11.37	0.00
Aminoacyl-tRNA biosynthesis	75	1	1.15E-05	11.37	0.00

Arginine and proline metabolism	77	3	4.80E-05	9.95	0.08
Glycine, serine and threonine metabolism	48	1	5.48E-03	5.21	0.05
Tyrosine metabolism	76	2	6.43E-03	5.05	1.9E-04
Ubiquinone and other terpenoid-quinone biosynthesis	36	1	1.05E-02	4.56	0.04

Supplemental Table T3. Summary of ROC curve analysis of 7 discriminant metabolites.

Metabolite A vs. B	AUC (95% CIs)	Optimal threshold	Sensitivity	Specificity
Citrulline	0.608 (0.367-0.850)	1.06	0.70	0.50
N-Acetylputrescine	0.658 (0.426-0.891)	1.24	0.70	0.58
N-Methyl-D-aspartic acid	0.729 (0.508-950)	1.90	0.70	0.67
N1,N12-Diacetylspermine	0.858 (0.705-1.000)	0.68	0.80	0.75
Lactic acid	0.817 (0.635-0.999)	0.92	0.80	0.67
Glycerol	0.833 (0.662-1.000)	0.88	0.80	0.75
5-Hydroxylysine	0.675 (0.425-0.925)	1.66	0.90	0.67
Metabolite A vs. C	**AUC (95% CIs)**	**Optimal threshold**	**Sensitivity**	**Specificity**
Citrulline	0.914 (0.777-1.000)	0.74	0.90	0.86
N-Acetylputrescine	0.857 (0.676-1.000)	1.01	0.90	0.71
N-Methyl-D-aspartic acid	0.879 (0.703-1.000)	1.64	0.80	0.86
N1,N12-Diacetylspermine	0.943 (0.824-1.000)	0.57	1.00	0.86
Lactic acid	0.929 (0.807-1.000)	0.91	0.80	0.86
Glycerol	0.900 (0.753-1.000)	0.86	0.80	0.86
5-Hydroxylysine	0.871 (0.703-1.000)	1.51	0.80	0.86
Metabolite B vs. C	**AUC (95% CIs)**	**Optimal threshold**	**Sensitivity**	**Specificity**
Citrulline	0.786 (0.576-0.996)	0.76	0.75	0.86
N-Acetylputrescine	0.690 (0.447-0.934)	1.04	0.67	0.71
N-Methyl-D-aspartic acid	0.744 (0.516-972)	1.35	0.67	0.71
N1,N12-Diacetylspermine	0.738 (0.489-0.987)	0.31	0.92	0.57
Lactic acid	0.560 (0.292-0.827)	0.72	0.58	0.57
Glycerol	0.631 (0.354-0.908)	0.54	0.75	0.57
5-Hydroxylysine	0.560 (0.276-0.843)	1.91	0.50	0.71

Supplemental Table T4. Summary of logistic regression models for predicting ASIA impairment grades using identified metabolites.*

		Predicted ASIA grade			
		A	B	C	Total
Observed ASIA grade	A	8	1	1	10
	B	2	8	2	12
	C	0	2	5	7
	Total	10	11	8	29

*The workflow and procedure used for generating the results in the table are shown below.

In the first step of analysis, logistic regression was conducted on the metabolites for evaluating binary classification of the injury severities A and non-A, and then a greedy stepwise backward selection was carried out on the samples of the data using the identified metabolites measurable in CSF and serum as well as their classes "A" and "non-A". The selection procedure produced a ranking of the importance of metabolites as a predictor of the injury severity in terms of A and non-A. The selected metabolites were citrulline, glycerol and N-methyl-D-aspartic acid in the first step of analysis.

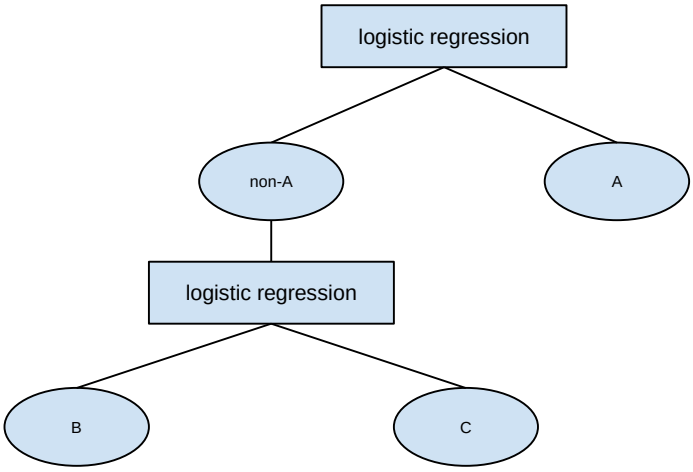

In the second step of analysis, logistic regression and greedy stepwise backward selection were conducted on the metabolites with patients of assigned grades "non-A" from the previous step. The selected metabolites were citrulline and glycerol in the second step. Logistic regression was conducted on the selected metabolites as a predictor for injury severity of B and C.

Below show the equations for generating the above table.

First step:

The logistic regression model with the selected metabolites as input variables x = (Citrulline, N-methyl-D-aspartic-acid, glycerol) learns their coefficients w = (2.5578, 1.9759, 5.916) and intercept 12.6459 and then calculates the class membership probability for A and NonA patients in the data set.

The hyperplane of all points x satisfying the equation $x' * w + intercept=0$ forms the *decision boundary* between the two classes, which is given by

x'w + intercept = 2.5578 * Citrulline + 1.9759 * (N-methyl-D-aspartic acid) + 5.916 * glycerol – 12.6459

Patients with 1 / (1 + exp(-x'w + intercept)) above the threshold of 0.5 were classified as A.

Second Step:

Likewise, in the second step, the logistic regression model with the selected metabolites as input variables x = (citrulline, glycerol) learns their coefficients w = (4.0015,3.4475) and the intercept - 5.2712 and then calculates the class membership probability for B and C patients in the data set.

P(B | x, w, intercept) = 1 / (1 + exp(-x'w + intercept));

P(C | x, w, intercept) = 1 - P(B | x, w, intercept).

where weighted_sum = x'w + intercept = 4.0015 * Citrulline + 3.4475 * glycerol - 5.2712

Patients with 1 / (1 + exp(-x'w + intercept)) above the threshold of 0.5 were classified as B.

Supplemental Table T5. Summary of logistic regression models for predicting ASIA impairment grades using putative metabolites in CSF.*

		Predicted ASIA grade			
		A	B	C	Total
Observed ASIA grade	A	9	0	1	10
	B	0	11	1	12
	C	0	0	7	7
	Total	9	11	9	29

*The number ID of putative metabolites used in the first step were C2717, C2094, C296, C114, C162 and C315, and in the second step were C1147, C3936 and C296.

The same two-step procedure as noted in Supplemental Table T3 was conducted on the putative metabolites in CSF for all patients.

Logistic Regression Equation for the above table:

First Step:

The logistic regression model with the top six selected metabolites as input variables x = (C2717, C2904, C296, C114, C162, C315) learns their coefficients w = (-83.435,15.3184,16.0929, 20.1932, -13.9344, 7.1853) and intercept -31.7988 and then calculates the class membership probability for A and NonA patients in the data set.

weighted_sum = x' w + intercept= -83.435 * C2717 + 15.3184 * C2904 + 16.0929 * C296 + 20.1932 * C114 + (-13.9344) * C162 + 7.1853 * C315 -31.7988

Patients with 1/(1 + exp(-weighted_sum)) above the threshold of 0.5 were classified as A; otherwise, non-A

Second Step:

In the second step, the logistic regression model with the selected metabolites as input variables x = (C1147, C3936, C296) learns their coefficients w = (96.9603,269.3487,-85.4335) and the intercept -204.4642 and then calculates the class membership probability for B and C patients in the data set.

weighted_sum = x' w + intercept = 96.9603* C1147 + 269.3487 * C3936 -85.4335 * C296 - 204.4642

Patients with 1/(1 + exp(-weighted_sum)) above 0.5 were classified as B; otherwise C.

Supplemental Table T6. Summary of logistic regression models for predicting ASIA impairment grades using putative metabolites in serum.*

		Predicted ASIA grade			
		A	B	C	Total
Observed ASIA grade	A	8	2	0	10
	B	0	12	0	12
	C	1	1	5	7
	Total	9	15	5	29

*The number ID of putative metabolites used in the first step were S15780, S2496 and S1053, and in the second step was S13214.

The same two-step procedure as noted in Supplemental Table T3 was conducted on the putative metabolites in serum for all patients.

Logistic Regression Equation for the above table:

First Step:

The logistic regression model with the top six selected metabolites as input variables x = (S15780, S2496, S1053) learns their coefficients w = (5.316, 1.7525, 1.3822) and intercept – 13.238 and then calculates the class membership probability for A and NonA patients in the data set.

weighted_sum = x'w + intercept = 5.316 * S15780 + 1.7525 * S2496 + 1.3822 * S1053 – 13.238

Patients with 1/(1 + exp(-weighted_sum)) above 0.5 were classified as class A; otherwise, non-A.

Second Step:

In the second step, the logistic regression model with the selected metabolites as input variables x = (S13214) learns their coefficients w = (-13.8837) and the intercept 24.8233 and then calculates the class membership probability for B and C patients in the data set.

weighted_sum = x w + intercept = -13.8837 * S13214 + 24.8233

Patients with 1/(1 + exp(-weighted_sum)) above the threshold of 0.5 were predicted as B; otherwise C.

Supplemental Table T7. Summary of logistic regression models for predicting ASIA impairment grades using putative metabolites in serum/CSF.*

		Predicted ASIA grade			
		A	B	C	Total
Observed ASIA grade	A	10	0	0	10
	B	1	11	0	12
	C	0	1	6	7
	Total	11	12	6	29

*The number ID of putative metabolites used in the first step were S15780, C4688, S2496, S143 and S984, and in the second step were S13214 and S984.

The same two-step procedure as noted in Supplemental Table T3 was conducted on the putative metabolites in both serum and CSF for all patients.

Logistic Regression Equation for the above table:

First Step:

The logistic regression model with the top six selected metabolites as input variables x = (S15780, C4688, S2496, S143, S984) learns their coefficients w = (61.739, 54.2275,23.431, 16.09, 62.5507) and intercept – 273.0694 and then calculates the class membership probability for A and NonA patients in the data set.

weighted_sum = x' w + intercept = 61.739 * S15780 + 54.2275 * C4688 + 23.431 * S2496 + 16.09 * S143 + 62.5507 * S984 – 273.0694

Patients with 1/(1 + exp(-weighted_sum)) above the threshold of 0.5 were predicted as A; otherwise Non-A

Second Step:

In the second step, the logistic regression model with the selected metabolites as input variables x = (S13214, S984) learns their coefficients w = (-326.8552, - 211.1922) and the intercept 758.648 and then calculates the class membership probability for B and C patients in the data set.

weighted_sum = x'w + intercept = -326.8552 * S13214 - 211.1922 * S984 + 758.648

Patients with 1/(1 + exp(-weighted_sum)) above the threshold of 0.5 were classified as B; otherwise, C.

Supplemental Table T8. List of top selected metabolites for building the prediction models.

Number ID	RT	Dansylated mass	Neutral mass	MCID with 0 reaction or HMDB*	# of matches in MCID with 1 reaction
C2717	11.46	409.1072	175.0489	2-Amino-3-oxoadipate	/
C2094	9.78	405.1174	342.1182	Disaccharide isomers such as sucrose	/
C296	3.25	355.1337	121.0754	/	21
C114	2.46	380.0813	146.023	/	29
C162	2.60	320.0443	85.98594	/	/
C315	3.34	558.1657	324.1074	/	31
C1147	7.30	337.1215	103.0632	b-aminoisobutyric acid N-Ethylglycine	/
C3936	14.49	518.1699	284.1115	/	18
C4688	15.61	308.0939	74.0356	3-Hydroxypropanal Lactaldehyde Hydroxyacetone	/
S15780	30.28	606.3466	372.2882	/	15
S2496	10.82	405.1484	171.0901	/	30
S1053	7.10	414.1203	180.0620	Monosaccharide isomers such as glucose	/
S13214	26.93	369.1021	270.0875	/	16
S143	2.54	295.114	61.0531	/	15
S984	6.92	707.1188	240.0095	/	/

*Accurate masses were first searched against the MyCompoundID database with zero reaction, which contain only endogenous metabolites. If there was no match, the accurate masses were then searched against the HMDB database. If there was still no match, MyCompoundID database with one reaction was used and the number of matches was listed in this table. Only metabolites with plausible structures (i.e., can be dansyl-labeled) were listed. Search criteria were mass error < 5 ppm. Some matches were excluded from the list because the retention time did not match with the dansyl standard library.